Studying the Cantor Dust at the Edge of Feigenbaum Diagrams

Aaron Klebanoff and John Rickert

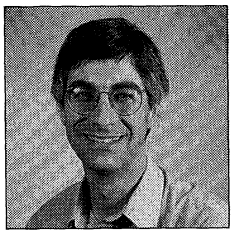

Aaron Klebanoff (aaron.klebanoff@rose-hulman.edu) received his Ph.D. in applied mathematics from the University of California at Davis in 1992. His interests include fractal geometry and chaotic dynamical systems, as well as anything else that spices up life in and out of the classroom. He has been a member of the mathematics department at Rose-Hulman Institute of Technology, a small engineering college in Terre Haute, Indiana, since 1993.

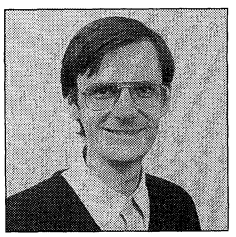

John Rickert (john.h.rickert@rose-hulman.edu) is an associate professor of mathematics at the Rose-Hulman Institute of Technology. He received his Ph.D. (1990) at the University of Michigan under the direction of David Masser. His main interests are diophantine equations, fostering student participation in mathematical competitions, and analysis of baseball statistics. He created the American Regions Math League home page and is a supporter of "Retrosheet."

Soon after Robert May [**4**], [**5**] first published results on the logistic maps $f_a : x \to ax(1-x)$, scientists began publishing diagrams like Figure 1 as evidence of *chaos*—a term coined in the early 1970s [**3**]. Such *Feigenbaum diagrams* (sometimes called *bifurcation diagrams*) are named after Mitchell Feigenbaum, who found that a large class of these diagrams have an amazingly simple relationship [**2**]. Figure 1 shows the asymptotic states for a typical orbit, at each parameter value a in $[1,4]$, by the following algorithm. For each value of a:

1. Pick a point x_0 in $(0,1)$. (Note that the point's orbit remains in $[0,1]$.)
2. Perform some number of iterations, say 1000, of f_a on x_0, and plot the last 500 values $\left(a, f_a^k(x_0)\right)$. (The more iterations the more accurate the diagram.)

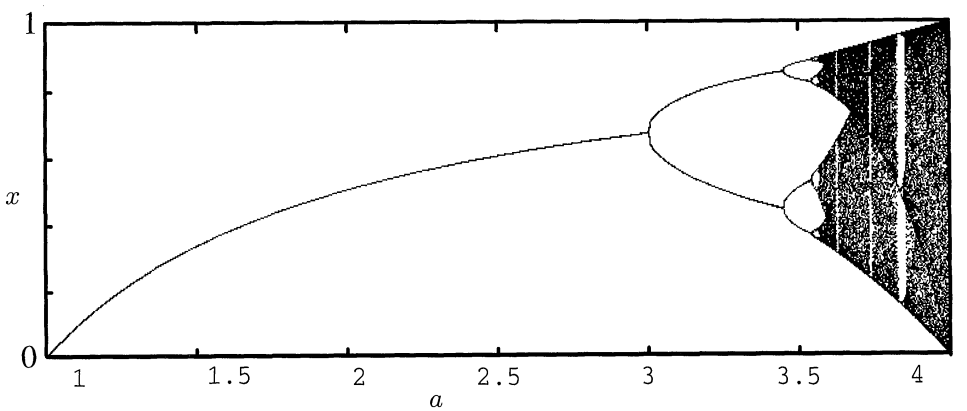

Figure 1. A Feigenbaum diagram for the logistic maps $f_a : x \to ax(1-x)$.

The Feigenbaum diagram for the logistic map shows the *period doubling regime*. For $a < 3$ all orbits are attracted to a fixed point, whose value increases from $x = 0$ for $a \leq 1$ to $x = 2/3$ for $a = 3$. As a increases beyond 3 the fixed point becomes repelling, but an absorbing 2-cycle appears in its place. Then, just beyond $a = 3.4$, the 2-cycle in turn becomes repelling but spawns an attracting 4-cycle, and so forth. For many larger values of a the orbit appears to be spread fairly evenly through a subinterval of $[0, 1]$—the successive iterates of x under the mapping jump chaotically about this subinterval. Finally, for $a = 4$, the orbit appears to be uniformly spread throughout the full unit interval. We will not be concerned here with the behavior of the orbits for $a \leq 4$, however, as this has been thoroughly studied elsewhere [**1**]. For $a > 4$, the orbits that remain in $[0, 1]$ form a set of measure 0; these orbits are too sparse to be visible in a computer display of the Feigenbaum diagram. We will focus our attention on the interesting behavior of the orbits here, for $a > 4$, beyond the edge of the Feigenbaum diagram.

To minimize the computational details, we will concentrate on a simpler family of maps, the *tent maps*, introducing a new diagram that will enable us to visualize the dynamics outside the parameter range covered by the Feigenbaum diagram. Once the properties of these *divergence diagrams* are understood, we will examine the divergence diagrams for the logistic maps and other well-known families of one-dimensional maps.

Tent Maps

The tent maps

$$T_c(x) = \begin{cases} 2cx & x \leq \frac{1}{2}, \\ 2c(1-x) & x > \frac{1}{2}, \end{cases}$$

can be thought of as a piecewise linear model of the logistic maps, as suggested by Figure 2. The graph of the tent map T_c looks like a clamped elastic string pulled up in the middle to the height c, and the logistic family stretches in a similar fashion as a increases.

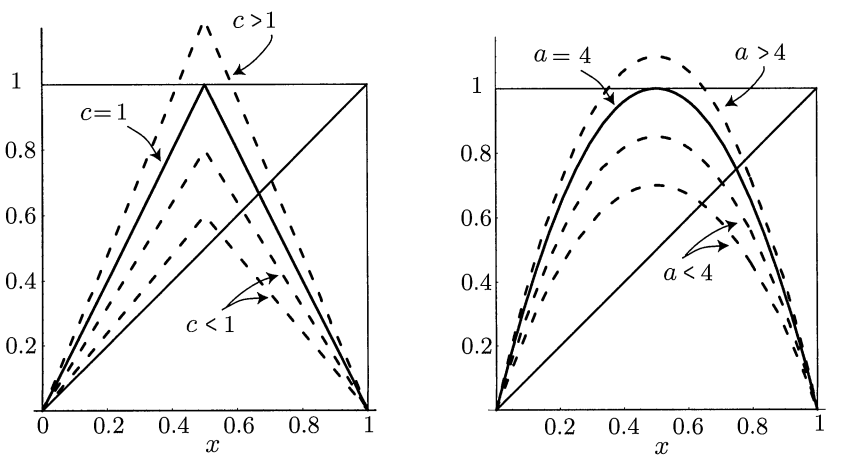

Figure 2. *Left,* typical tent maps $T_c(x)$. *Right,* typical logistic maps $f_a(x)$.

A convenient way to study an orbit of a one-dimensional map such as T_c is to make a *web diagram*. We plot the graph of $y = T_c(x)$ and the line $y = x$ together, using the line to display the outputs of the map, which become the inputs for the following iteration. That is, we indicate the orbit of a point x_0 in $[0, 1]$ by drawing first a vertical segment from x_0 to the graph of T_c, then a horizontal segment from $\big(x_0, T_c(x_0)\big)$ to the line $y = x$, and again a vertical segment from $\big(T_c(x_0), T_c(x_0)\big)$ to the graph, and so on. The resulting trail of vertical and horizontal segments allows a viewer to easily follow the orbit. We focus on the unit interval $0 \le x \le 1$ because the orbits under T_c of points in the unit interval remain in this interval, for all c-values between 0 and 1; that is, $T_c([0, 1]) \subseteq [0, 1]$.

Figure 3 shows sample web diagrams for tent maps with various values of the parameter c between 0 and 1. When $c < 0.5$, all orbits are attracted to the origin; when $c = 0.5$, all points on $\left[0, \frac{1}{2}\right]$ are fixed and the others are fixed after one iteration.

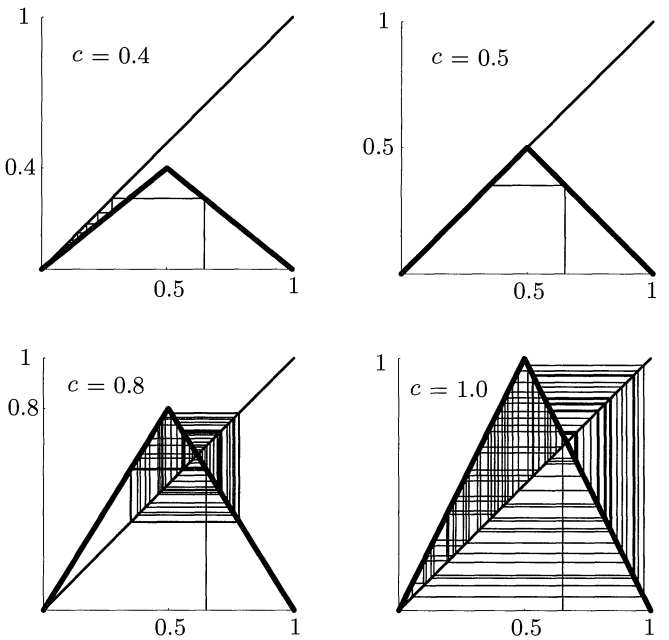

Figure 3. Web diagrams for some tent maps.

It is when $\frac{1}{2} < c \le 1$ that the dynamics suddenly become quite complicated. The slopes of the graphs of T_c and of all iterates $T_c^n = T_c \circ T_c \circ \cdots \circ T_c$ are greater than 1 in magnitude, so there are no attracting periodic orbits. As a result, the tent maps become chaotic, as shown in Figure 4, without the familiar period doubling found with the logistic maps. The curves $x = c$ and $x = 2c(1 - c)$ form upper and lower bounds for the diagram on $\frac{1}{2} < c \le 1$.

The tent map with $c > 1$. What happens when the value of c is greater than 1? As c approaches 1 from the left, the Feigenbaum diagram (Figure 4) shows chaotic orbits spanning the x-interval $[0, 1]$. When $c > 1$, graphical analysis is helpful for

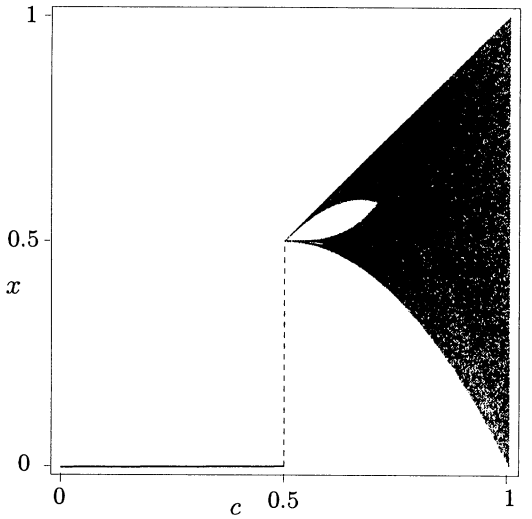

Figure 4. Feigenbaum diagram for the family of tent maps.

understanding the fate of orbits of the tent maps. Figure 5 shows the web diagram for the case $c = \frac{3}{2}$.

Notice that for $c > 1$ the apex of the "tent" exceeds 1, and if $T_c(x) > 1$ the orbit of x will exit the unit interval, never to return. For this reason, we find that the first iteration of T_c removes points in the open segment of length $1 - (1/c)$ in the middle of the x-interval $[0, 1]$; only the two closed end segments each of length $1/(2c)$ remain in $[0, 1]$ after a single iteration of T_c. In turn, the points in the middle of these two subintervals exit the unit interval upon another iteration of T_c. This process continues, leaving 2^n disjoint closed subintervals of $[0, 1]$, each of length $1/(2c)^n$, whose image under T_c^n remains in $[0, 1]$. The points of $[0, 1]$ whose orbits under the tent map T_c remain in $[0, 1]$ form a Cantor set $\mathcal{C}_c$; the classic "middle-thirds" Cantor set is $\mathcal{C}_{3/2}$.

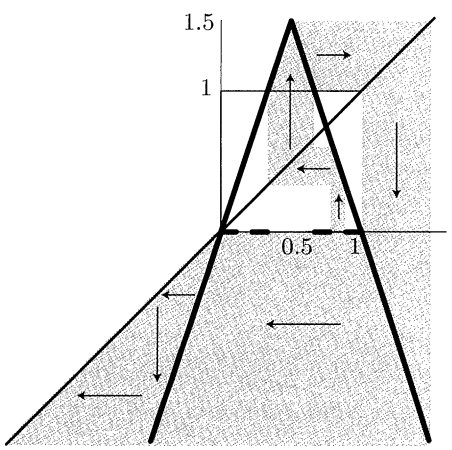

Figure 5. Web diagram for the tent map $T_{3/2}(x)$.

Now we know why the Feigenbaum diagram in Figure 4 stops at $c = 1$. For $c > 1$ almost all orbits diverge to $-\infty$; only Cantor sets $\mathcal{C}_c$ are left invariant under T_c. But Cantor sets have measure 0, so they cannot be shown realistically on a computer screen—the term *Cantor dust* suggests their appearance. (The dynamical behavior of the tent map for the special case $c = \frac{3}{2}$ is described carefully, using only the simplest tools, in [**6**]. There the dynamics are used to deduce the main topological features of the classic Cantor "middle-thirds" set $\mathcal{C}_{3/2}$.)

We can visualize the spectrum of invariant Cantor sets $\mathcal{C}_c$ by using a graphing technique usually reserved for complex maps. We know that if any orbit of T_c attains a value greater than 1, then it must ultimately diverge, and almost all orbits do diverge. So for each point x corresponding to a parameter value c, we color or shade the point in the cx-plane according to how many iterations $x \to T_c(x) \to T_c^2(x) \to \cdots$ it takes to exceed the bound $x = 1$. If x is already greater than 1, we make the point (c, x) white. If the orbit exceeds 1 after a single iteration, we shade the point (c, x) a light gray. The point (c, x) is progressively darkened the more iterations it takes for the orbit to exceed 1, and it is made black if more than, say, 10 iterations are required to exceed this bound. (Modern computers can handle far more than 10 iterations, but the graphs don't appear much different when larger numbers are used.) We call the resulting graph a *divergence diagram*. It extends the range of c in which we can display the limiting behavior of the orbits for the tent family, and it provides a visual description of the way the fractal dimension of the invariant Cantor sets varies with this parameter. A divergence diagram for the tent map is shown in Figure 6.

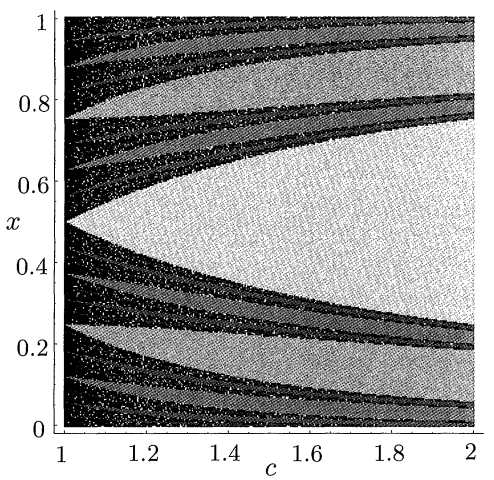

Figure 6. Divergence diagram for the tent map.

Since n iterations of the tent map leaves 2^n disjoint closed sub-intervals of $[0, 1]$, each of length $1/(2c)^n$, the fractal (Hausdorff) dimension of $\mathcal{C}_c$ is easily computed:

$$\dim \mathcal{C}_c = \frac{\log 2}{\log 2 + \log c}.$$

As Figure 6 suggests, this formula tells us that when $c = 1$ the dimension is 1, and as c increases fractal dimension decreases.

Looking at the divergence diagrams, it is tempting to find out more. The curved boundaries in the diagram occur at the edges of the intervals that are mapped out of the unit square. The largest region leaves in one iteration and is bounded by the curves

$$x_{1_1}(c) = \frac{1}{2c} \quad \text{and} \quad x_{1_2}(c) = 1 - \frac{1}{2c}$$

which satisfy $T_c(x) = 1$. In fact, while tedious, it is not hard to compute the other boundaries. We will call the boundary between the regions in which iterates escape in n iterations x_n, and we will further sub-index for the 2^n such curves. For example, when $T_c(x) = x_{1_i}$ we obtain four boundary curves for the regions in which the orbits escape in two iterations:

$$x_{2_{(1,1)}} = \frac{1}{4c^2}, \qquad x_{2_{(1,2)}} = 1 - \frac{1}{4c^2},$$
$$x_{2_{(2,1)}} = \frac{1}{2c} - \frac{1}{4c^2}, \qquad x_{2_{(2,2)}} = 1 - \frac{1}{2c} + \frac{1}{4c^2}.$$

We find the other boundary curves recursively by applying

$$x_{n_{(i_1,i_2,\ldots,i_j)}} = \begin{cases} \dfrac{1}{2c} x_{(n-1)_{(i_1,i_2,\ldots,i_{j-1})}} & \text{if } i_j = 1, \\ 1 - \dfrac{1}{2c} x_{(n-1)_{(i_1,i_2,\ldots,i_{j-1})}} & \text{if } i_j = 2. \end{cases}$$

Equipped with these formulas, we can easily determine the width of the bands removed after n iterations to be $(2c-2)/(2c)^n$. From this, we find that the nth band is widest when $c = n/(n-1)$. It is worth noting that the symmetry in the tent maps is apparent in the divergence diagram, yet not at all clear from the Feigenbaum diagram.

There are rich dynamics beyond $c = 1$, and here it is easiest to link chaotic dynamics with fractals. When $c > 1$, the tent map stretches and folds the unit interval with each iteration, which mixes points just as kneading mixes bread dough. The Cantor sets $\mathcal{C}_c$ are fractals that are invariant under the tent map, and the dynamics of the map are intimately connected with the topological structure of the Cantor sets [6]. To summarize, $\mathcal{C}_c$ contains points whose orbits are dense; that is, points whose orbits come arbitrarily close to all points in $\mathcal{C}_c$. On the other hand, the periodic points are dense in in $\mathcal{C}_c$, so that arbitrarily close to any point there is a periodic point—a point whose orbit returns to its start after a finite number of iterations of the tent map. Finally, the tent map has *sensitive dependence on initial conditions* in $\mathcal{C}_c$—arbitrarily close to any point x_0 in this set there is a point x_1 such that for some n the separation $|T_c^n(x_1) - T_c^n(x_0)|$ exceeds the fixed bound $1/(2c)$. In brief, the dynamics of the tent map T_c on the Cantor set $\mathcal{C}_c$ are *chaotic*.

The tent map with $c < 0$. What happens when c is negative? Figure 7 shows some typical orbits in three qualitatively different cases. For $-1 \le c < -\frac{1}{2}$, typical orbits are chaotic on $\left[c, 2c^2\right]$. When $c = -\frac{1}{2}$, 0 is the only fixed point and all other integers are eventually fixed at 0. All points $x \in \left[-\frac{1}{2}, 0\right) \cup \left(0, \frac{1}{2}\right]$ are period 2 points and the rest of the nonintegers are eventually period 2. For $-\frac{1}{2} < c < 0$, all orbits are attracted to 0.

The square region $S = I \times I$ where $I = [1/(2c+1), 2c/(2c+1)]$ contains the vertex of the tent map when $c \ge -1$. In this case, I is invariant under T_c (i.e.,

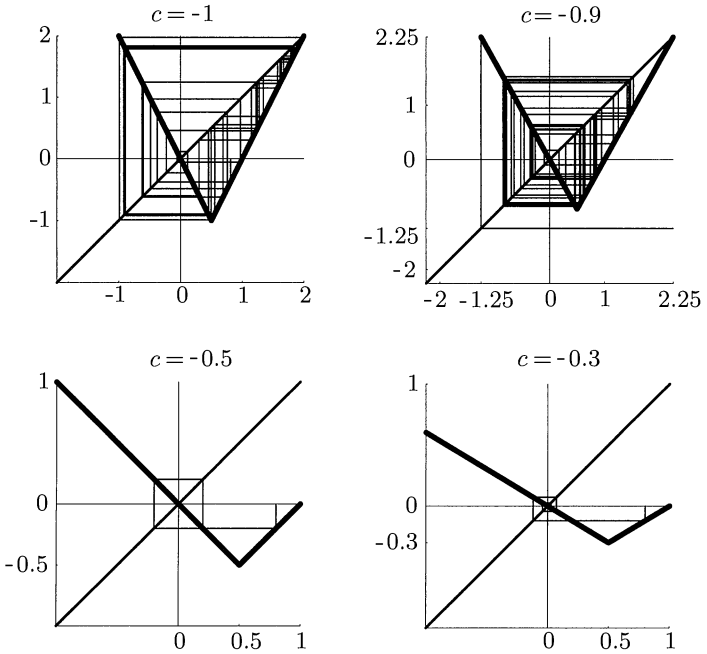

Figure 7. Web diagrams for some tent maps.

$T_c(I) \subset I$), and the attractor is bounded by the interval $[c, 2c^2]$. However, once $c < -1$, the vertex of the tent map emerges from S, resulting in Cantor sets. So, to create a divergence diagram for $c < 0$, rather than waiting until points leave $[0, 1]$ as we did when $c > 0$, we now count iterations until they leave the interval I.

Figure 8 shows a complete picture for the dynamics of the tent family by providing both a divergence diagram and a Feigenbaum diagram to represent the dynamics for all values of c and x. Note that the two diagrams are complementary; the Feigenbaum diagram indicates the structure of the bounded orbits for $|c| \leq 1$ values where the divergence diagram gives little information. But the divergence diagram shows the behavior of orbits near the invariant Cantor sets $\mathcal{C}_c$, for $|c| \geq 1$, beyond the ends of the Feigenbaum diagram.

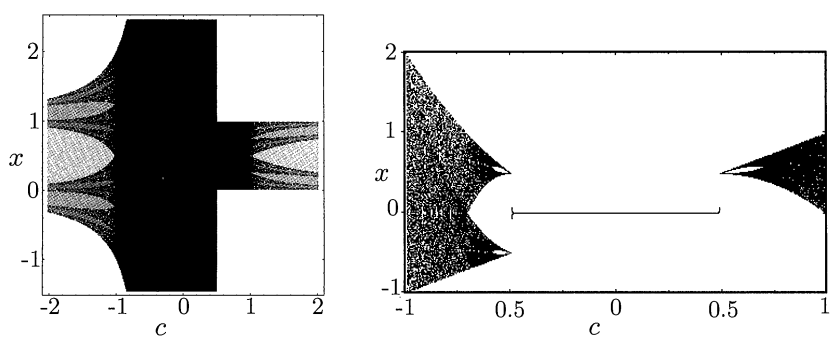

Figure 8. Divergence and Feigenbaum diagrams for the tent maps.

The Logistic Family

We return to the logistic family $f_a(x) = ax(1-x)$ by thinking of it as a smooth version of the tent family (Figure 2). As a is increased from 0 to 4, the behavior of the orbits is similar to what we found when we increased the parameter c in the tent map from 0 to 1. For both families of maps, when the parameter is small, orbits originating in $[0,1]$ tend to 0, and for large parameter values, the mappings exhibit chaos. Comparing the Feigenbaum diagrams in Figures 1 and 4, we are reminded that the paths to chaos are quite different. Nevertheless, the divergence diagrams, Figures 6 and 9, show that the dynamics of the logistic maps for $a > 4$ and the tent maps for $c > 1$ have many features in common.

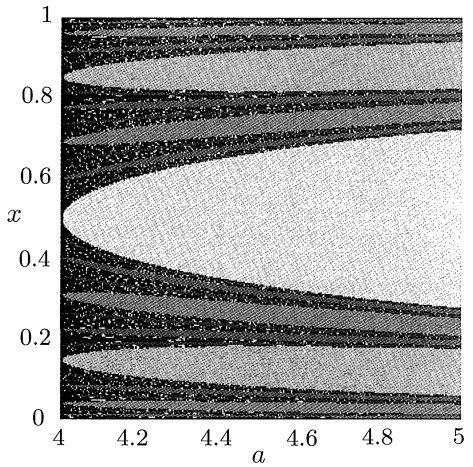

Figure 9. Divergence diagram for the logistic maps.

The curved boundaries in the diagram are (not surprisingly) similar to the tent map's. The largest region leaves in one iteration and is bounded by the curves

$$x_{1_i} = \frac{1}{2} + (-1)^i \sqrt{\frac{1}{4} - \frac{1}{a}}, \qquad i = 1, 2,$$

which satisfy $f_a(x) = 1$. Much as we labeled boundary curves in the tent divergence diagram, we now index the boundary curves of the regions in which iterates escape in n iterations by x_n, further sub-indexing for the 2^n such curves. When $f_a(x) = x_{1_i}$ we obtain the boundary curves for the regions in which the orbits escape in two iterations,

$$x_{2_{(i,j)}} = \frac{1}{2}(-1)^i \sqrt{\frac{1}{4} - \frac{1}{2a} + \frac{(-1)^j}{a}\sqrt{\frac{1}{4} - \frac{1}{a}}}, \qquad i, j = 1, 2.$$

We find the other boundary curves recursively by applying

$$x_{n_{(i,j,k,\ldots)}} = \frac{1}{2} + (-1)^i \sqrt{\frac{1}{4} - \frac{1}{a} x_{(n-1)_{(j,k,\ldots)}}}, \qquad i, j, k, \ldots = 1, 2.$$

We can use these curves to obtain estimates of the fractal dimensions of the Cantor sets. These formulas make it reasonably easy to check that after one iteration, the

width of the intervals left behind is asymptotic to $1/a$. After n iterations, with the aid of a computer algebra system, we can verify that the width of the 2^n intervals left behind is asymptotic to $1/a^n$. So, the fractal dimension of the invariant Cantor sets for the logistic maps is asymptotic to $\log 2/\log a$ as a tends to infinity. Note that this coincides with the asymptotic result for the tent family!

Conclusion. While Feigenbaum diagrams typically focus our attention on period-doubling routes to chaos, the divergence diagram focuses our attention on the invariant Cantor sets (on which the maps act chaotically) and their fractal dimensions. The black central region in a divergence diagram is the home of the Feigenbaum diagram. Feigenbaum diagrams are both beautiful and useful tools for showing the limiting behavior of bounded orbits of one-dimensional maps. However, these diagrams do not capture the dynamics on Cantor sets that commonly arise in chaotic one-dimensional dynamical systems. The large white regions in the divergence diagram are the abyss into which most orbits diverge, but the banded structure that remains helps us to visualize the invariant Cantor sets where the interesting dynamics occurs.

For complex maps, the Mandelbrot and Julia sets yield comparable pictures of the dynamics. The Mandelbrot set shows for which values of the complex parameter typical orbits diverge, and the Julia set for the map with a fixed parameter value shows the set of points whose orbits diverge. In fact, if the Mandelbrot and Julia sets for a complex map could be combined in a four-dimensional plot, our divergence diagram for the associated real map would be the projection from the cartesian product of the two complex planes onto the real plane.

With this in mind, we end by showing in Figure 10 the divergence and Feigenbaum diagrams for the quadratic family, $Q_b(x) = x^2+b$, with which the original Mandelbrot set is associated. The Feigenbaum diagrams for the quadratic and logistic family are strikingly similar. However, their divergence diagrams illuminate a key distinction by showing how the bounds on the Cantor sets change with the parameter in the quadratic family. As with the other examples, the symmetry in the maps is reflected in the divergence diagrams.

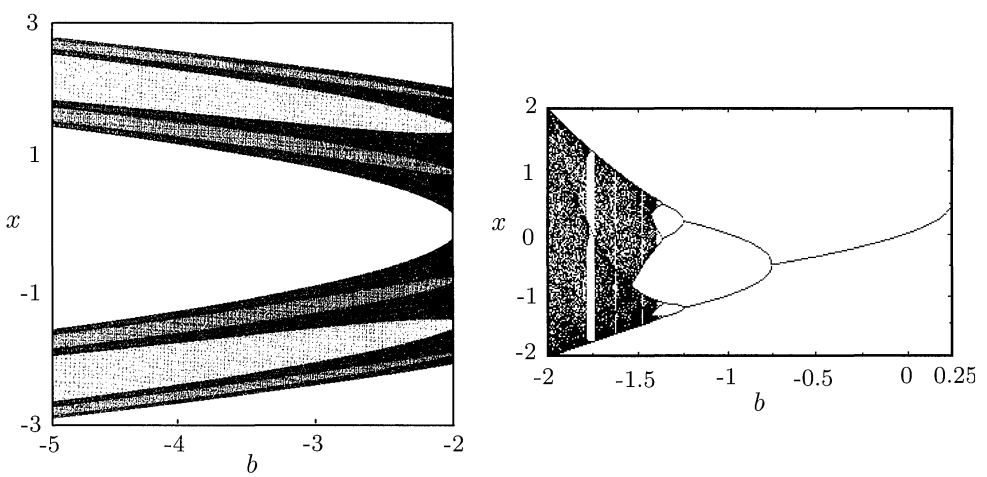

Figure 10. Feigenbaum and divergence diagrams for the quadratic family.

We affectionately call the divergence diagram for the quadratic family *Cantor's comet*; see Figure 11. The black region (the head of the comet) contains the Feigenbaum diagram, and only points within this black region will work as seeds for generating the Feigenbaum diagram.

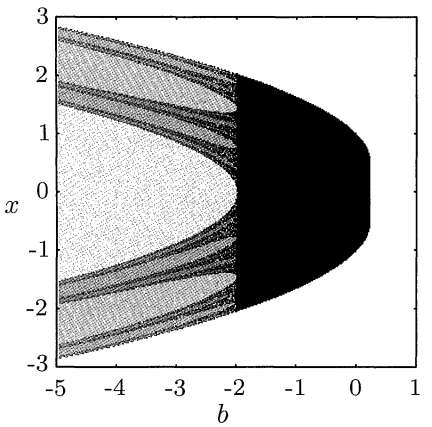

Figure 11. Cantor's comet.

Acknowledgment. We thank our reviewers for many helpful comments; Cary Laxer for the use of the excellent facilities in the Imaging Laboratory at Rose-Hulman; and Robert Devaney for helpful conversations.

References

1. R. L. Devaney, *An Introduction to Chaotic Dynamical Systems*, 2nd ed., Addison-Wesley, Menlo Park, CA, 1989.
2. M. J. Feigenbaum, Quantitative universality for a class of nonlinear transformations, *Journal of Statistical Physics* 19 (1978) 25–52.
3. T.-Y. Li and J. A. Yorke, Period three implies chaos *American Mathematical Monthly* 82 (1975) 985–992.
4. R. M. May, Biological populations with non-overlapping generations: Stable points, stable cycles and chaos, *Science* 186 (1974) 645–647.
5. ———, Simple mathematical models with very complicated dynamics, *Journal of Theoretical Biology* 51 (1976) 511–524.
6. W. C. Mercier, How chaotic things work, *College Mathematics Journal* 28:2 (1997) 110–118.